Return period and risk analysis of nonstationary low-flow series under climate change

Return Period and Risk Analysis of Nonstationary Low-flow Series

Tao Du[1], Lihua Xiong[1*], Chong-Yu Xu[1,2], Christopher James Gippel[3], Shenglian Guo[1,4], Pan Liu[1]

[1]*State Key Laboratory of Water Resources and Hydropower Engineering Science, Wuhan University, Wuhan 430072, China*

[2]*Department of Geosciences, University of Oslo, P.O. Box 1022 Blindern, N-0315 Oslo, Norway*

[3]*Australian Rivers Institute, Griffith University, Nathan, Queensland 4111, Australia*

[4]*Hubei Provincial Collaborative Innovation Center for Water Resources Security, Wuhan University, Wuhan 430072, China*

E-mail addresses:

T. Du (dtgege@126.com),

L. Xiong (xionglh@whu.edu.cn),

C-Y. Xu (c.y.xu@geo.uio.no),

C.J. Gippel (fluvialsystems@fastmail.net),

S. Guo (slguo@whu.edu.cn),

P. Liu (liupan@whu.edu.cn),

* Corresponding author:

Lihua Xiong, PhD, Professor

State Key Laboratory of Water Resources and Hydropower Engineering Science

Wuhan University, Wuhan 430072

People's Republic of China

E-mail: xionglh@whu.edu.cn

Telephone: +86-13871078660

Fax: +86-27-68773568

Return Period and Risk Analysis of Nonstationary Low-flow Series

Abstract The concept of return period and the associated risk of occurrence of extreme events are critical considerations in the management of water resources. A precondition for conducting hydrological frequency analysis to estimate return period and risk is the assumption of stationarity of the hydrological variable of interest, but this is problematic because climate change and human activities can act to make hydrological phenomena nonstationary. Two different interpretations of return period, i.e. the expected waiting time (EWT) and expected number of exceedances (ENE), have been proposed to consider nonstationarity in return period and risk analysis by introducing the time-varying moments method into nonstationary frequency analysis, under the assumption that the statistical parameters are functions only of time. This paper explored the use of meteorological variables to improve the characterization of nonstationary return period and risk under the ENE interpretation by employing meteorological covariates in the nonstationary frequency analysis. The advantage is that the downscaled future meteorological variables from the General Circulation Model (GCM) outputs can be used to calculate the statistical parameters and exceedance probabilities for future years. The EWT interpretation using time as covariate was also applied for comparison. Both interpretations of return period were applied to the low-flow (annual minimum monthly streamflow) series of the Wei River, China. Both interpretations gave an estimate of nonstationary return period and risk that was significantly different from the stationary case. The nonstationary return period and risk under ENE interpretation using temperature and precipitation as covariates were more reasonable and advisable than those of the EWT case using time as covariate. We concluded that nonstationary analysis can improve decision making in the management of water resources of the Wei River basin during dry seasons exacerbated by climate change.

Keywords return period; risk; nonstationarity; low-flow; General Circulation Model (GCM)

1 Introduction

Statistical inference is used in hydrological frequency analysis under the assumption that hydrological events such as flood and drought are randomly distributed through time. A precondition for traditional frequency analysis is the assumption of stationarity, which means that controlling environmental factors such as climate and land cover act to generate or modify the hydrological variable of interest in the same way in the past, present and future (Gilroy and McCuen, 2012; Katz, 2013). However, under the conditions of climate change, land use change and river regulation, acting individually or together, the assumption of stationarity is suspect (Katz et al., 2002; Xiong and Guo, 2004; Milly et al., 2005; Milly et al., 2008). To overcome this problem, various approaches have been developed for conducting nonstationary hydrological frequency analysis (Khaliq et al., 2006). The concept of event return period (or recurrence interval) and the associated risk of occurrence, with potential consequences of loss of life, social disruption, economic loss and ecological disturbance, are critical considerations in the management of water resources, especially with regard to design and operation of hydraulic structures in rivers. Under nonstationary conditions, estimates of return period and risk are ambiguous unless the temporally changing environment is explicitly considered in the analysis.

The most common way of handling nonstationarity in hydrological time series data is the method of time-varying moments, which assumes that although the distribution function type of the hydrological variable of interest remains the same, the statistical parameters are time-varying (Strupczewski et al., 2001; Coles, 2001; Katz et al., 2002; Villarini et al., 2009; Gilroy and McCuen, 2012; Jiang et al., 2014). With the method of time-varying moments, it is not difficult to derive an annual value of the return period of a hydrological event given a specific design quantile (Olsen et al., 1998; Villarini et al., 2009), i.e. $T_t = 1/p_t = 1/(1-F_Z(z_{p_0}, \theta_t))$, where T_t and p_t are the annual return period and exceedance probability, respectively, of the given design quantile z_{p_0} with fitted yearly statistical parameters θ_t, and F_Z is the

cumulative distribution function of the hydrological event of interest. However, for many planning and design applications, a measure of return period that varies from one year to the next is impractical. To deal with this issue, various studies have been carried out for return period estimation and risk analysis that consider nonstationary conditions (Wigley, 1988, 2009; Olsen et al., 1998; Parey et al., 2007, 2010; Cooley, 2013; Salas and Obeysekera, 2014). Among these various studies to return period and risk estimation under nonstationary conditions two different interpretations of return period are used. The first is that the expected waiting time (EWT) until the next exceedance event is T years (Wigley, 1988, 2009; Olsen et al., 1998; Cooley, 2013; Salas and Obeysekera, 2014), and the second is that the expected number of exceedances (ENE) of the event in T years is 1 (Parey et al., 2007, 2010; Cooley, 2013). These two interpretations will be referred to here as EWT and ENE.

An early study by Wigley (1988), later revisited (Wigley, 2009), used the EWT interpretation to consider how nonstationarity can be included in the concepts of return period and risk of extreme events. A normal distribution with a linear increasing trend in the mean was assumed, and the changes in the return period and risk were derived by the technique of stochastic simulation. Building on this work, Olsen et al. (1998) presented a more rigorous mathematical examination of the effect of nonstationarity on the concepts of return period and risk, also using the EWT interpretation. Parey et al. (2007, 2010) introduced the ENE interpretation into the nonstationary framework to derive air temperature return levels in France. A detailed review and comparison of the two interpretations of return period can be found in Cooley (2013). Recently, Salas and Obeysekera (2014) extended the geometric distribution to allow for changing exceedance probabilities over time, considering the cases of increasing, decreasing and shifting extreme events. Although these studies vary, they have in common the assumption that the statistical parameters are functions only of time. However, this carries the unreasonable implication that the identified pattern of nonstationarity in a hydrological time series will continue indefinitely. Also, while runoff can follow inter-year cyclical patterns, the lack of a direct physical link between time and runoff means that time is not useful as an explanatory variable.

The time-varying moments method can be extended to perform covariate analysis by replacing time with any physical factors that are known to be causative of the hydrological variable of interest. Using meteorological variables as covariates could be more effective and have greater physical meaning for modeling return period and risk under nonstationary conditions than simply using time as covariate. This physical covariate analysis approach has previously been explored for nonstationary frequency analysis of extreme events (Coles, 2001; Villarini et al., 2010; López and Francés, 2013), but to our knowledge has not been incorporated with either the EWT or ENE interpretation of return period and applied to estimating return period and risk of extreme events under nonstationary conditions.

Like many other places around the world, in China hydrological processes are under the influence of climate change and large-scale anthropogenic activities, so the assumption of stationarity of river flow series is not valid for many rivers, with most exhibiting decreasing trends (Zhang et al., 2011). The Wei River, the largest tributary of the Yellow River, is the major source of water supply for the economic hub of Western China – the Guanzhong Plain. The Wei River basin is one of the most important industrial and agricultural production zones in China. However, in recent decades the Wei River basin has suffered a significant decrease in streamflow (Song et al., 2007; Zuo et al., 2014), which threatens industrial and agricultural production and socioeconomic development. The increasing scarcity of water resources under conditions of climate change is a serious cause for concern not only in the Wei River basin, but across the entire nation. There is an urgent need to provide water resource managers and policy makers with reliable information on the return period and risk characteristics of the low-flow component of the flow regime of the Wei River under the prevailing nonstationary conditions.

The aim of this paper is to use data from the Wei River basin to investigate the concepts of return period and risk of the low-flow component, defined here by the annual minimum monthly streamflow, under a nonstationary framework. We eschew the traditional assumption of increasing, decreasing or shifting statistical parameters with time (e.g. Salas and Obeysekera, 2014) and alternatively employ meteorological

covariate analysis in the nonstationary frequency analysis of the low-flow series. General Circulation Model (GCM) outputs provide the statistical parameters of the nonstationary low-flow distribution by substituting downscaled meteorological variables into the derived optimal nonstationary model with meteorological covariates to extend the exceedance probabilities into the future. GCM outputs are temporally finite which does not suit the EWT interpretation of return period, so this paper adopts the ENE interpretation in development of the new approach. The EWT interpretation of return period using time as covariate is also applied in this study for the purpose of comparison with the new approach.

This paper first describes the Wei River basin and the available data sets used in the study. Then the methods for determining the return periods (under the EWT and ENE interpretations) and risk under stationary and nonstationary conditions are described, along with a brief outline of the methods of nonstationary frequency analysis of the low-flow series using time-varying moments, and statistical downscaling of meteorological variables. The results and discussion of the Wei River case study follow, and finally we make conclusions about the performance of our proposed approach in the case study and its potential for wider application.

2 Study area and data

2.1 General characteristics of the study area

The Wei River, the largest tributary of the Yellow River, originates from the Niaoshu Mountain at an elevation of 3 485 m above sea level in the Weiyuan county of Gansu province. The Wei River has a length of 818 km and a drainage area of 134 800 km^2, covering the coordinates of 33°40′-37°26′N, 103°57′-110°27′E in the southeastern part of the loess plateau (Fig. 1). The river flows through three provinces (autonomous region) of Gansu, Ningxia and Shanxi from west to east, and joins the Yellow River at Tongguan in Shanxi province. The Wei River has two large tributaries, the Jing River and the Beiluo River, located in the middle and lower reaches of the basin, respectively (Fig. 1). The Wei River is known regionally as the ‘Mother River’

of the Guanzhong Plain of the southern part of the loess plateau because of its key role in the economic development of western China (Song et al., 2007; Zuo et al., 2014).

The Wei River basin is characterized by semi-arid and sub-humid continental monsoon climate. Average annual precipitation of the basin is about 570 mm, but there is a strong decreasing gradient from south to north. The southern region has a sub-humid climate with annual precipitation usually within the range 800-1000 mm, whereas the northern region has a semi-arid climate with annual precipitation usually within the range 400-700 mm. The annual average temperature over the entire basin ranges from 6 to 14ºC. The range in the annual potential evapotranspiration is 660-1600 mm, and the basin average annual actual evapotranspiration from the land surface is about 500 mm.

The average annual natural discharge of the Wei River is about 10×10^9 m^3, contributing approximately 17% of the discharge of the Yellow River. The annual discharge of the Wei River at Linjiacun station during the decade 1991-2000 was 53.9% less than that during the preceding decade, while at Huaxian station near the basin outlet it was 50.3% less (Song et al., 2007). This reduction has been attributed to a combination of natural factors and human activities (McVicar et al., 2007; Song et al., 2007).

2.2 Data

Three kinds of data were used in this study: observed hydrological data, observed meteorological data, and NOAA National Centers for Environmental Prediction (NCEP) reanalysis data and GCM outputs of the Coupled Model Intercomparison Project Phase 5 (CMIP5).

Observed mean daily streamflow data from Huaxian gauging station (Fig. 1) over the period 1954-2009, provided by the Hydrology Bureau of the Yellow River Conservancy Commission, was the source of the low-flow series, defined here as the annual minimum monthly streamflow (Fig. 2). Huaxian hydrological station, located at 109°46′E, 34°35′N, is about 70 km upstream of the junction of the Wei and Yellow

rivers (Fig. 1). The catchment area upstream of this station is 106 500 km^2, or about 80% of the total basin area.

Temperature and precipitation are two meteorological variables that are closely related to streamflow and were chosen as covariates for nonstationary frequency analysis of low-flow. Observed daily average temperature and daily total precipitation series from 22 stations (Fig. 1) for the period 1954-2009 were obtained from the National Climate Center of the China Meteorological Administration (source: http://cdc.cma.gov.cn). The areal average daily series of both variables for the basin above Huaxian station were generated using the Thiessen polygon method, and from these the annual average temperature and annual total precipitation series (denoted by T_{ave} and Pr, respectively) over the period of 1954-2009 were extracted.

The NCEP reanalysis daily data and GCM daily data were employed to derive the future temperature and precipitation scenarios using the statistical downscaling technique (Wilby et al., 2002, 2007). The 26 candidate predictors of NCEP reanalysis data as described in Wilby and Dawson (2007) for the period of 1954-2009 were obtained from the NOAA Earth System Research Laboratory (ESRL) (source: http://www.esrl.noaa.gov). The Representative Concentration Pathways (RCPs) are four greenhouse gas concentration and emissions pathways adopted by the IPCC for its fifth Assessment Report (AR5), each one named according to radiative forcing target level in watts per square metre for year 2100 (van Vuuren et al., 2011). For this paper we used RCP8.5 scenario, which represents the upper bound of the RCPs, but future work could extend our analysis by examining the other RCPs with smaller radiative forcing target levels. RCP8.5 scenario is characterized by increasing greenhouse gas emissions over time, representative of scenarios in the literature that lead to comparatively high greenhouse gas concentration levels, and does not include any specific climate mitigation target (Riahi et al., 2011). The same 26 predictors of seven different GCMs (CanESM2, CNRM-CM5, GFDL-ESM2M, NorESM1-M, MIROC-ESM, MIROC-ESM-CHEM, CCSM4) under the RCP8.5 scenario for the period of 2010-2099 inclusive were obtained from the CMIP5 (source:

http://cmip-pcmdi.llnl.gov/cmip5). The NCEP and GCM data are gridded to different spatial scales, so data preprocessing was necessary. First, predictors of both data sets were interpolated to each meteorological site. Then, areal average series of every predictor for the basin above Huaxian station were calculated using the Thiessen polygon method.

3 Methodology

Firstly, the exceedance probability of a low-flow event, which is the key element for determining the return period and risk, is defined. Then, theories about the return periods (under the EWT and ENE interpretations) and risk of a low-flow event concerning the future exceedance probability under stationary and nonstationary conditions are described. Finally, in deriving the future exceedance probability for the determination of the nonstationary return period and risk of a low-flow event, the time-varying moments method is employed in the nonstationary frequency analysis of the observed low-flow series by using time or meteorological variables as covariates. When using meteorological variables as covariates, the downscaled future meteorological variables from the GCM outputs can be used to calculate the statistical parameters and exceedance probabilities for future years. For the sake of completeness, the methods used in this chapter are briefly described in the following subsections.

3.1 Exceedance probability of low-flow event

The low-flow character of the flow regime is denoted by the random variable Z. Our interest is on the scarcity of water resources, so we define the design low-flow quantile z_{p_0} for which in any given year has a probability p_0 that the streamflow is lower than this quantile (Fig. 3). The probability of a flood event that is higher than a design flood quantile is usually referred to as the exceedance probability, or as the exceeding probability (e.g. Salas and Obeysekera, 2014). In the case of low-flow (drought) event, the meaning of exceedance or exceeding is that the drought severity

is exceeded, or the value of the flow statistic is lower than the design quantile.

Under stationary conditions, the cumulative distribution function of Z is denoted by $F_Z(z|\boldsymbol{\theta})$, where $\boldsymbol{\theta}$ is the constant statistical parameter set. At an initial year $t=0$ (which normally refers to the last observed year), given an initial return period T_0 and corresponding exceedance probability $p_0 = 1/T_0$, the design low-flow quantile can be derived from $z_{p_0} = F_Z^{-1}(p_0, \boldsymbol{\theta})$, where F_Z^{-1} is the inverse function of F_Z. In the stationary case, since the $\boldsymbol{\theta}$ is constant for every year, the exceedance probability corresponding to the design quantile z_{p_0} is p_0 for each future year (Fig. 3), which can be obtained by:

$$p_t = F_Z(z_{p_0}, \boldsymbol{\theta}) = p_0, \quad t = 1, 2, ..., \infty \tag{1}$$

Under nonstationary conditions, the cumulative distribution function of Z is denoted by $F_Z(z|\boldsymbol{\theta}_t)$, where $\boldsymbol{\theta}_t$ varies in accordance with time or, more directly, with meteorological variables. In nonstationary case, the design low-flow quantile corresponding to the initial exceedance probability $p_0 = 1/T_0$ can be derived from $z_{p_0} = F_Z^{-1}(p_0, \boldsymbol{\theta}_0)$, where $\boldsymbol{\theta}_0$ is the statistical parameter set of the initial year $t=0$. The statistical parameters are time-varying so the future exceedance probability corresponding to z_{p_0} is not constant any more. In this case, the temporal variation in the exceedance probability corresponding to z_{p_0} can be characterized by the way the low-flow distribution or, more specifically, the statistical parameters change through time (Fig. 4). The exceedance probability for each future year can be obtained by:

$$p_t = F_Z(z_{p_0}, \boldsymbol{\theta}_t), \quad t = 1, 2, ..., \infty \tag{2}$$

3.2 Return period using EWT interpretation

Under stationary conditions, if X is denoted as the random variable representing the year of the first occurrence of a low-flow that exceeds (i.e. is lower

than) the design quantile, then a low-flow Z exceeding the design value z_{p_0} for the first time in year $X = x, x = 1, 2, ..., \infty$, follows the geometric probability law (Mood et al., 1974; Salas and Obeysekera, 2014):

$$f(x) = P(X = x) = (1 - p_0)^{x-1} p_0, \quad x = 1, 2, ..., \infty \tag{3}$$

Noting that Eq. 3 is derived on the assumptions of independence and stationarity, then the expected value of X, i.e. the return period (expected waiting time interpretation) of the low-flow exceeding the design quantile z_{p_0} under stationary conditions, is:

$$T = E(X) = \sum_{x=1}^{\infty} x f(x) = 1 / p_0 \tag{4}$$

Under nonstationary conditions, the exceedance probability corresponding to z_{p_0} is no longer constant (Fig. 4), and then the geometric probability law considering time-varying exceedance probabilities p_t is (Cooley, 2013; Salas and Obeysekera, 2014):

$$f(x) = P(X = x) = (1 - p_1)(1 - p_2)...(1 - p_{x-1}) p_x = p_x \prod_{t=1}^{x-1} (1 - p_t), \quad x = 1, 2, ..., \infty \tag{5}$$

The EWT-return period T of the low-flow exceeding the design quantile z_{p_0} under nonstationary conditions is thus:

$$T = E(X) = \sum_{x=1}^{\infty} x f(x) = \sum_{x=1}^{\infty} x p_x \prod_{t=1}^{x-1} (1 - p_t) \tag{6}$$

3.3 Return period using ENE interpretation

Under stationary conditions, if M is denoted as the random variable representing the number of exceedances in T years, then $M = \sum_{t=1}^{T} I(Z_t < z_{p_0})$, where $I()$ is the indicator function. M follows a binomial distribution (Cooley, 2013):

$$f(m) = P(M = m) = \binom{T}{m} p_0^m (1 - p_0)^{T-m} \tag{7}$$

It follows that the expected value of M is 1:

$$E(M) = \sum_{t=1}^{T} p_0 = T p_0 = 1 \tag{8}$$

And thus the return period (expected number of exceedances interpretation) of the low-flow exceeding the design quantile z_{p_0} under stationary conditions is $T = 1/p_0$.

Under nonstationary conditions, the exceedance probability is not constant and M does not follow a binomial distribution. In this situation the expected number of exceedances is expressed as (Cooley, 2013):

$$E(M) = \sum_{t=1}^{T} E[I(Z_t < z_{p_0})] = \sum_{t=1}^{T} P(Z_t < z_{p_0}) = \sum_{t=1}^{T} F_Z(z_{p_0}, \boldsymbol{\theta}_t) = \sum_{t=1}^{T} p_t \tag{9}$$

The ENE-return period T of the low-flow exceeding the design quantile z_{p_0} under nonstationary conditions can thus be derived by setting Eq. 9 equal to 1 and solving:

$$\sum_{t=1}^{T} p_t = 1 \tag{10}$$

3.4 Hydrological risk

In practical application of hydrological frequency analysis, the management question is often framed as one of risk, whereby, for a design life of n years, the hydrological risk R is the probability of a low-flow event exceeding the design value z_{p_0} before or at year n. This risk can be derived from the perspective of complement, which means that there is no exceedance during the design life of n years. Under the assumption of independence and stationarity, the probability of the complement is $(1 - p_0)^n$. Then the hydrological risk under stationary conditions is:

$$R = 1 - (1 - p_0)^n \tag{11}$$

Likewise, for a design life of n years, the probability of a low-flow exceeding the design quantile z_{p_0} before or at year n under the circumstances of time-varying

exceedance probabilities p_t is:

$$R = 1 - [(1 - p_1)(1 - p_2)...(1 - p_n)] = 1 - \prod_{t=1}^{n} (1 - p_t) \quad (12)$$

3.5 Nonstationary frequency analysis of low-flow series

The standard was of calculating the nonstationary return periods under the EWT and ENE interpretations and the risk of a design quantile z_{p_0} corresponding to an initial return period T_0 is by Eq. 6, Eq. 10 and Eq. 12, respectively. An important part of the procedure is derivation of time-varying exceedance probabilities p_t (Eq. 2) for future years. This relies on determination of the relationships of the statistical parameters of the low-flow distribution to the explanatory variables, which is normally referred to as nonstationary frequency analysis. Several studies have explored nonstationary return period and risk analysis of extreme events using only time as covariate in the nonstationary frequency analysis (Wigley, 1988, 2009; Olsen et al., 1998; Parey et al., 2007, 2010; Cooley, 2013; Salas and Obeysekera, 2014). Unlike time as covariate, meteorological variables have physical meaning and therefore explanatory power. Thus, in the method presented here, we derive the time-varying exceedance probabilities p_t for future years by employing meteorological covariates in the nonstationary frequency analysis of low-flow events. The future meteorological time series data were derived from statistical downscaling of GCM outputs. The ENE interpretation was adopted in development of this new approach, as the GCM outputs extend into the future for a finite time period.

The nonstationary low-flow series was modeled using the time-varying moments method, which was built under the Generalized Additive Models in Location, Scale and Shape (GAMLSS) framework (Rigby and Stasinopoulos, 2005; Xiong et al., 2014). Five distribution functions widely used in modeling low-flow data were considered as candidates (Table 1): Gamma (GA), Weibull (WEI), Gumbel (GU), Logistic (LO), and Lognormal (LOGNO). Nonstationarities in both the location μ

and scale σ parameters were examined through monotonic link functions $g(\cdot)$ (Table 1) and the optimal nonstationary model was selected by penalizing more complex models in terms of the Akaike Information Criterion (AIC) (Akaike, 1974). The model with the smallest AIC value was considered the optimal one. While the AIC value identifies the optimal model, it is not a measure of model performance. Goodness-of-fit of the selected optimal model was assessed qualitatively by the worm (Buuren and Fredriks, 2001) and the centile curves diagnostic plots, and quantitatively using the statistics of the Filliben correlation coefficient (denoted by F_r) (Filliben, 1975) and the Kolmogorov-Smirnov (KS) test (denoted by D_{KS}) (Massey, 1951).

To summarize, the main steps in deriving time-varying exceedance probabilities p_t for future years are: (i) nonstationary modeling of the observed low-flow series by using time (for EWT interpretation) or meteorological variables (for ENE interpretation) as covariates, (ii) calculating the design low-flow quantile z_{p_0} corresponding to an initial return period T_0 from the quantile function $z_{p_0} = F_Z^{-1}(p_0, \boldsymbol{\theta}_0)$, where $p_0 = 1/T_0$, $\boldsymbol{\theta}_0$ is the fitted statistical parameter set of the initial year $t = 0$, and F_Z^{-1} is the inverse function of F_Z, and (iii) deriving time-varying exceedance probabilities p_t corresponding to z_{p_0} from $p_t = F_Z(z_{p_0}, \boldsymbol{\theta}_t)$ for future years $t = 1, 2, ..., \infty$ (for EWT interpretation) or $t = 1, 2, ..., t_{\max}$ (for ENE interpretation), where $\boldsymbol{\theta}_t$ is the future statistical parameter set derived either directly from the optimal nonstationary model of step (i) using time as covariate or from the optimal nonstationary model of step (i) using meteorological variables as covariates into which the downscaled future meteorological variables are substituted.

3.6 Statistical downscaling model (SDSM)

The General Circulation Model (GCM) is a tool for predicting future time series

of meteorological variables, thereby extending the time-varying exceedance probabilities of Eq. 10 and Eq. 12. The coarse spatial resolution of GCM data restricts its direct application to local impact studies (Wilby et al., 2002, 2007), but this problem can be overcome by a technique known as downscaling. The statistical downscaling model (SDSM) provided by Wilby et al. (2002) is a decision support tool for assessing local climate change impacts using a robust statistical downscaling technique that combines a weather generator and multiple linear regression. SDSM has been widely used in research related to climate change (Wilby and Dawson, 2013) and is fully described in Wilby et al. (2002) and Wilby and Dawson (2007).

The future scenarios of T_{ave} and Pr were projected using the SDSM with the NCEP reanalysis data and the seven GCM outputs of CMIP5. Following the advice of Wilby and Dawson (2007) and Hessami et al. (2008), the five predictors mean sea level pressure, 500 hPa geopotential height, 500 hPa eastward wind, 850 hPa air temperature, and near-surface air temperature, were selected for the downscaling of T_{ave} and one additional predictor, 850 hPa specific humidity, was included for Pr. Multiple linear regression equations for both daily average temperature and daily total precipitation were optimized with the respective selected large-scale NCEP reanalysis predictors. Then, daily average temperature and daily total precipitation for the period of 1954-2009 were simulated by the weather generator in the SDSM driven by the NCEP reanalysis predictors. As the statistics of annual average temperature T_{ave} and annual total precipitation Pr, rather than daily data, were used in the nonstationary frequency analysis of low-flow, the simulation results were assessed by the Nash-Sutcliffe efficiency (NSE) between the simulated and observed T_{ave} and Pr. Daily average temperature and daily total precipitation for the period of 2010-2099 generated by the scenario generator in the SDSM driven by the GCM predictors were used to calculate the statistics of T_{ave} and Pr for the future years of 2010-2099 for the seven GCM models.

4 Results and discussion

4.1 Nonstationary frequency analysis of low-flow series

The observed low-flow magnitude declined through time, with irregular scatter (Fig. 2). A significant decreasing trend was detected by the Mann-Kendall test (Mann, 1945; Kendall, 1975; Li et al., 2014) with the statistic $Z_{MK} = -2.71$ compared to the critical value of $Z_{1-\alpha/2} = 1.96$ at $\alpha = 0.05$. More detailed analysis of this nonstationarity was undertaken as part of modeling the low-flow series under the GAMLSS framework.

When the low-flow series was modeled using time as covariate, the AIC values suggested that the Weibull distribution (WEI) (with logarithmic link functions for both the location μ and scale σ parameters) was the optimal distribution, with both parameters modeled as linear functions of time (Fig. 5a). This was selected as the optimal nonstationary model using time as covariate.

Almost all of the worm points were within the 95% confidence intervals (Fig. 6a), indicating good consistency between the selected model and the observed low-flow data. The vast majority of the points were within the 5% and 95% centile curves (Fig. 6b) indicating that the model captured the variability of the data. The statistics of the F_r and the D_{KS} (Table 2) also indicated that the selected nonstationary model was an adequate fit to the low-flow series.

In fitting the low-flow series to nonstationary models with the annual average temperature T_{ave} and annual total precipitation Pr as covariates, the most complex model expressed both statistical parameters μ and σ as linear functions of T_{ave} and Pr. This process also involved all possible simpler sub-models. As for the model with time as covariate, the AIC values also suggested that the WEI distribution (with logarithmic link functions for both the location μ and scale σ parameters) was the optimal distribution, with μ and σ modeled as linear functions of T_{ave} and Pr,

respectively (Fig. 5b). This was selected as the optimal nonstationary model using meteorological variables as covariates.

All the worm points were within the 95% confidence intervals, indicating perfect consistency between the selected model and the observed low-flow data (Fig. 7a). The vast majority of the points were within the 5% and 95% centile curves (Fig. 7b) indicating that the model captured the variability of the data. The statistics of the F_r and the D_{KS} (Table 2) also indicated that the selected nonstationary model was an adequate fit to the low-flow series. In addition, the optimal nonstationary model using T_{ave} and Pr as covariates had a smaller AIC value than the optimal model using time as covariate (Fig. 5 and Table 2), suggesting it was the superior approach.

4.2 Statistical downscaling of temperature and precipitation

For the optimal nonstationary model with T_{ave} and Pr as covariates, the future time series of these two variables allowed calculation of the time-varying parameters μ_t and σ_t for future years, enabling estimation of the time-varying exceedance probabilities p_t into the future. The Nash-Sutcliffe efficiency (NSE) between the simulated and observed T_{ave} and Pr (Fig. 8) suggested an adequate result for T_{ave}, but the result for Pr was not as good. This was expected, as it is acknowledged that the downscaling of precipitation is more problematic than temperature. As other authors have done in similar situations (Wilby and Dawson, 2007; Chen et al., 2012; Yang et al., 2012), we considered the simulation result acceptable for this purpose.

The projected annual time series of T_{ave} and Pr for the future period 2010-2099 for the seven GCM models (Fig. 9) showed a strong increasing trend for T_{ave} (around 0.056°C per year for the ensemble average), while the ensemble average value of Pr was stable at around 470 mm.

4.3 EWT-return period and risk under nonstationarity

Under the EWT interpretation of return period, having determined the optimal nonstationary model using time as covariate with estimated parameters μ_0 and σ_0 (Table 2), the nonstationary return period T of the design low-flow quantile z_{p_0} corresponding to the specified initial return period T_0 was computed using Eq. 6. The nonstationary return period T of z_{p_0} was much shorter than the specified T_0 (Fig. 10a). For example, when $T_0 = 50$ years, the value of T under nonstationarity was only 18.6 years. The implication is that for a design low-flow quantile z_{p_0}, if stationarity was incorrectly assumed, a low-flow lower than z_{p_0} would be expected to occur about 50 years after the initial year $t = 0$. Using 50 years as the basis for water resources planning decisions for this exceedance event would be imprudent because nonstationarity of the low-flow series suggests that 19 years is more appropriate.

Given the initial return period T_0 and design life n, the hydrological risk R of the design low-flow quantile z_{p_0} for stationary and nonstationary conditions was calculated using Eq. 11 and Eq. 12, respectively (Fig. 10b). Under both cases risk increased with n, but for any T_0, the R for nonstationary conditions was higher than the R for stationary conditions. For example, when $T_0 = 50$ and $n = 40$ years, the risks for the stationary and nonstationary conditions were 55.4% and 96.8%, respectively (Fig. 10b). The implication is that, for a design low-flow quantile z_{p_0} corresponding to $T_0 = 50$, if stationarity was incorrectly assumed, the probability of low-flow event lower than z_{p_0} occurring before or at year $n = 40$ would be 55.4%, whereas in reality, because of nonstationarity, the probability would be 96.8%.

4.4 ENE-return period and risk under nonstationarity

Under the ENE interpretation of return period, having determined the optimal nonstationary model using temperature and precipitation as covariates with estimated parameters μ_0 and σ_0 (Table 2) and downscaled future T_{ave} and Pr, the nonstationary return period T of the design low-flow quantile z_{p_0} corresponding to the specified initial return period T_0 was computed using Eq. 10. The comparison of T and T_0 under the ENE interpretation (Fig. 11a) was quite different to that under the EWT interpretation (Fig. 10a). In the case of the ENE interpretation, for $T_0 < 20$, the nonstationary T was slightly longer than the stationary T_0, while for $T_0 \geq 20$, the nonstationary T was shorter than the stationary T_0 (Fig. 11a), but to a lesser degree than for the EWT interpretation (Fig. 10a). For example, when $T_0 = 10$ years, the value of T under the correct assumption of nonstationarity was 12 years, while when $T_0 = 50$ years, the value of T under the correct assumption of nonstationarity was 33 years. In this case, the implications for water resources planning decisions based on an incorrect assumption of stationarity would depend on the magnitude of T_0 (z_{p_0}).

Given the initial return period T_0 and design life n, the hydrological risk R of the design low-flow quantile z_{p_0} for stationary and nonstationary conditions was calculated using Eq. 11 and Eq. 12, respectively (Fig. 11b). The result was similar to that for the return period (Fig. 11a). For $n < 20$, the R for nonstationary conditions was slightly lower than the R for stationary conditions, while for $n \geq 20$, the R for nonstationary conditions was higher than the R for stationary conditions. For example, when $T_0 = 50$ and $n = 10$ years, the risks for the stationary and nonstationary conditions were 18.3% and 14.1%, respectively. The implication is that,

for a design low-flow quantile z_{p_0} corresponding to $T_0 = 50$, if stationarity was incorrectly assumed, the risk of a low-flow event lower than z_{p_0} occurring before or at year $n = 10$ would be 18.3%, whereas in reality, because of nonstationarity, the probability of this event was 14.1%. In contrast, when $T_0 = 50$ and $n = 40$ years, the nonstationary risk probability was 79.0%, which was much higher than the stationary case of 55.4%. In this case, the implications for risk associated with water resources planning based on an incorrect assumption of stationarity would depend on the chosen design life n.

4.5 Discussion

The nonstationary return periods and risks of low-flow events for both interpretations of return period (EWT and ENE) were clearly different from those where the incorrect assumption of stationarity was applied for the purpose of comparison (Fig. 10 and Fig. 11). This result demonstrates the importance of considering nonstationarity when estimating return period and hydrological risk. There were also large differences between the results for the two interpretations of return period under the nonstationary framework.

For the EWT interpretation, which uses time as covariate, both the nonstationary return period and hydrological risk values suggest that, in the future, the occurrence of low-flow events will be a more serious problem compared with that suggested by analysis based on the assumption of stationarity (Fig. 10). For the ENE interpretation, which uses temperature and precipitation as covariates in the nonstationary model, the comparison of return period and risk of low-flow events with the stationary model depends on the magnitude of the design low-flow quantile and the length of the design life (Fig. 11). Under the EWT interpretation, the fitted model location μ and scale σ parameters monotonously decrease with time (Fig. 12a, b), which results in a relatively small value of design low-flow z_{p_0} corresponding to specific T_0 (Fig. 12c). However, there has been a noticeable upward movement in the annual minimum

monthly streamflow since the mid-1990s (Fig. 2), which contradicts the patterns of sustained decrease in the model statistical parameters over time (Fig. 12a, b). Therefore, simply using time as covariate and assuming indefinite decreasing trends in the statistical parameters is inappropriate. In contrast, the ENE interpretation, which uses temperature and precipitation as covariates, provides better model performance (Fig. 6, Fig. 7 and Table 2), more reasonable statistical parameters (Fig. 12a, b) and realistic design low-flow (Fig. 12c). Overall, the analysis suggests that the nonstationary return period and risk of a low-flow event derived by a model that includes meteorological variables would produce more reliable information to assist decision making in the management of water resources during naturally dry periods that are being progressively exacerbated over time by the effects of climate change.

5 Conclusions

Two interpretations of return period, i.e. the expected waiting time (EWT) and expected number of exceedances (ENE), were considered to explore the return period and risk of a low-flow event in the Wei River, China under nonstationary conditions. Under the ENE interpretation, meteorological variables were employed in the nonstationary frequency analysis and downscaled future meteorological variables from the GCM outputs were used for deriving the future statistical parameters of the low-flow distribution and further the exceedance probabilities for future years. This approach was compared with the EWT interpretation, which used time as covariate in the frequency analysis. A number of conclusions were drawn from this study that have implications for assessing risk in water resources management in the common situation of nonstationary river flow data.

The Weibull distribution (with logarithmic link functions for the two model parameters) was the best distribution for modeling the observed low-flow series for the Wei River. Significant nonstationarities were detected in both model parameters. For the EWT interpretation using time as covariate, the optimal nonstationary model expressed both model parameters as linear functions of time, and for the ENE interpretation using meteorological variables as covariates, the optimal nonstationary

model expressed both model parameters as linear functions of annual average temperature and annual total precipitation, respectively. The optimal nonstationary model of using meteorological variables as covariates performed better than that of the case using time as covariate.

For the EWT interpretation, there were significant differences between the nonstationary return period and risk of a low-flow event and those corresponding to the stationary conditions. The nonstationary return period was much shorter (more frequent event occurrence) than the stationary case, indicating that the scarcity of water resources during dry seasons will worsen over time. However, this result may overstate the risk of a low-flow event due to inappropriate fitted statistical parameters. There is evidence of an increase in low-flow events since the mid-1990s, but the nonstationary return period and risk were derived under the assumption that both model parameters monotonously decrease indefinitely. In contrast, the ENE interpretation, where the model used the physical variables temperature and precipitation as covariates, provided more appropriate fitted statistical parameters and thus more reasonable and plausible nonstationary estimates of return period and risk. On the basis of the Wei River data, the ENE nonstationary analysis of return period and risk is recommended for generating information to assist decision making for the management of water resources during dry seasons exacerbated by climate change. This conclusion is likely to apply to the many similar situations around the world.

The conclusion of this study that the nonstationary return period and risk of low-flow event based on the ENE interpretation was more advisable than that based on the EWT interpretation might not apply universally. We used only one of the four Representative Concentration Pathways adopted by the IPCC for its fifth Assessment Report, and future research could consider the others, which have smaller radiative forcing target levels. Uncertainties exist in the downscaled future scenarios of meteorological variables used here, and this could be partly addressed by exploring more downscaling methods and GCM models. Further work is needed to investigate the uncertainty of the design low-flow quantile and how this affects uncertainty of the estimates of nonstationary return period and risk.

Acknowledgements

This research is financially supported by the National Natural Science Foundation of China (Grants NSFC 51190094 and NSFC 51479139), which are gratefully acknowledged. The contribution of CJG was made whilst visiting the College of Water Resources and Hydropower Engineering, Wuhan University, supported by the High-End Foreign Expert Recruitment Programme, administered by the State Administration of Foreign Experts Affairs, Central People's Government of the People's Republic of China.

References

Akaike H (1974) A new look at the statistical model identification. IEEE T Automat Contr 19 (6): 716-723. http://dx.doi.org/10.1109/TAC.1974.1100705

Buuren SV, Fredriks M (2001) Worm plot: a simple diagnostic device for modelling growth reference curves. Stat Med 20 (8): 1259-1277. http://dx.doi.org/10.1002/sim.746

Chen H, Xu C-Y, Guo SL (2012) Comparison and evaluation of multiple GCMs, statistical downscaling and hydrological models in the study of climate change impacts on runoff. J Hydrol 434-435: 36-45. http://dx.doi.org/10.1016/j.jhydrol.2012.02.040

Coles S (2001) An introduction to statistical modeling of extreme values. Springer, London. http://dx.doi.org/10.1007/978-1-4471-3675-0

Cooley D (2013) Return periods and return levels under climate change. In: AghaKouchak, A., Easterling, D., Hsu, K., Schubert, S., Sorooshian, S., (eds.) Extremes in a changing climate. Springer, Dordrecht, Netherlands. http://dx.doi.org/10.1007/978-94-007-4479-0_2

Filliben JJ (1975) The probability plot correlation coefficient test for normality. Technometrics 17 (1): 111-117. http://dx.doi.org/10.1080/00401706.1975.10489279

Hessami M, Gachon P, Ouarda TBMJ, St-Hilaire André (2008) Automated regression-based statistical downscaling tool. Environ Modell Softw 23 (6): 813-834. http://dx.doi.org/10.1016/j.envsoft.2007.10.004

Gilroy KL, McCuen RH (2012) A non-stationary flood frequency analysis method to adjust for future climate change and urbanization. J Hydrol 414: 40-48.

http://dx.doi.org/10.1016/j.jhydrol.2011.10.009

Jiang C, Xiong LH, Xu C-Y, Guo SL (2014) Bivariate frequency analysis of nonstationary low-flow series based on the time-varying copula. Hydrol Process. http://dx.doi.org/10.1002/hyp.10288

Katz RW, Parlang MB, Naveau P (2002) Statistics of extremes in hydrology. Adv Water Resour 25 (8): 1287-1304. http://dx.doi.org/10.1016/S0309-1708(02)00056-8

Katz RW (2013) Statistical methods for non-stationary extremes. In: AghaKouchak, A., Easterling, D., Hsu, K., Schubert, S., Sorooshian, S., (eds.) Extremes in a changing climate. Springer, Dordrecht, Netherlands. http://dx.doi.org/10.1007/978-94-007-4479-0_2

Kendall MG (1975) Rank correlation methods. London: Griffin

Khaliq MN, Ouarda TBMJ, Ondo JC, Gachon P, Bobée B (2006) Frequency analysis of a sequence of dependent and/or non-stationary hydro-meteorological observations: A review. J Hydrol 329 (3): 534-552. http://dx.doi.org/10.1016/j.jhydrol.2006.03.004

Li DF, Xie HT, Xiong LH (2014) Temporal change analysis based on data characteristics and nonparametric test. Water Resour Manage 28: 227-240. http://dx.doi.org/10.1007/s11269-013-0481-2

López J, Francés F (2013) Non-stationary flood frequency analysis in continental Spanish rivers, using climate and reservoir indices as external covariates. Hydrol Earth Syst Sci 17: 3189-3203. http://dx.doi.org/10.5194/hess-17-3189-2013

Mann HB (1945) Nonparametric tests against trend. Econometrica 13 (3): 245-259. http://www.jstor.org/stable/1907187

Massey FJ Jr (1951) The Kolmogorov-Smirnov test for goodness of fit. J Am Stat Assoc 46 (253): 68-78. http://dx.doi.org/10.1080/01621459.1951.10500769

McVicar TR, Li L, Van Niel TG, Zhang L, Li R, Yang Q, Gao P (2007) Developing a decision support tool for China's re-vegetation program: Simulating regional impacts of afforestation on average annual streamflow in the Loess Plateau. Forest Ecol Manag 251 (1): 65-81. http://dx.doi.org/10.1016/j.foreco.2007.06.025

Milly PCD, Betancourt J, Falkenmark M, Hirsch RM, Kundzewicz ZW, Lettenmaier DP, Stouffer RJ (2008) Stationarity is dead: whiter water management? Science 319 (5863): 573-574. http://dx.doi.org/10.1126/science.1151915

Milly PCD, Dunne KA, Vecchia AV (2005) Global pattern of trends in streamflow and water availability in a changing climate. Nature 438 (7066): 347-350. http://dx.doi.org/10.1038/nature04312

Olsen JR, Lambert JH, Haimes YY (1998) Risk of extreme events under nonstationary conditions. Risk Anal 18 (4): 497-510. http://dx.doi.org/10.1111/j.1539-6924.1998.tb00364.x

Parey S, Malek F, Laurent C, Dacunha-Castelle D (2007) Trends and climate evolution: statistical approach for very high temperatures in France. Climatic Change 81(3-4): 331-352. http://dx.doi.org/10.1007/s10584-006-9116-4

Parey S, Hoang TTH, Dacunha-Castelle D (2010) Different ways to compute temperature return levels in the climate change context. Environmetrics 21: 698-718. http://dx.doi.org/10.1002/env.1060

Riahi K, Rao S, Krey V, Cho C, Chirkov V, Fischer G, Kindermann G, Nakicenovic N, Rafaj P (2011) RCP 8.5 – A scenario of comparatively high greenhouse gas emissions. Climatic Change, 109: 33-57. http://dx.doi.org/10.1007/s10584-011-0149-y

Rigby RA, Stasinopoulos DM (2005) Generalized additive models for location, scale and shape. J Roy Stat Soc C-App 54 (3): 507-554. http://dx.doi.org/10.1111/j.1467-9876.2005.00510.x

Salas JD, Obeysekera J (2014) Revisiting the concepts of return period and risk for non-stationary hydrologic extreme events. J Hydrol Eng 19: 554-568. http://dx.doi.org/10.1061/(ASCE)HE.1943-5584.0000820

Song J, Xu Z, Liu C, Li H (2007) Ecological and environmental instream flow requirements for the Wei River-the largest tributary of the Yellow River. Hydrol Process 21: 1066-1073. http://dx.doi.org/10.1002/hyp.6287

Strupczewski WG, Singh VP, Feluch W (2001) Non-stationary approach to at-site flood frequency modeling I. Maximum likelihood estimation. J Hydrol 248 (1-4): 123-142. http://dx.doi.org/10.1016/S0022-1694(01)00397-3

van Vuuren DP, Edmonds J, Kainuma M, Riahi K, Thomson A, Hibbard K, Hurtt GC, Kram T, Krey V, Lamarque J-F, Masui T, Meinshausen M, Nakicenovic N, Smith SJ, Rose SK (2011) The representative concentration pathways: an overview. Climatic Change, 109: 5-31. http://dx.doi.org/10.1007/s10584-011-0148-z

Villarini G, Smith JA, Serinaldi F, Bales J, Bates PD (2009) Flood frequency analysis for

non-stationary annual peak records in an urban drainage basin. Adv Water Resour 32 (8): 1255-1266. http://dx.doi.org/10.1016/j.advwatres.2009.05.003

Villarini G, Smith JA, Napolitano F (2010) Non-stationary modeling of a long record of rainfall and temperature over Rome. Adv Water Resour 33 (10): 1256-1267. http://dx.doi.org/10.1016/j.advwatres.2010.03.013

Wigley TML (1988) The effect of climate change on the frequency of absolute extreme events. Clim Monit 17(1-2): 44-55.

Wigley TML (2009) The effect of changing climate on the frequency of absolute extreme events. Climatic Change 97(1-2): 67-76. http://dx.doi.org/10.1007/s10584-009-9654-7

Wilby RL, Dawson CW, Barrow EM (2002) SDSM – a decision support tool for the assessment of regional climate change impacts. Environ Modell Softw 17: 147-159.

Wilby RL, Dawson CW (2007) SDSM 4.2 – a decision support tool for the assessment of regional climate change impacts. User Manual.

Wilby RL, Dawson CW (2013) The Statistical DownScaling Model: insights from one decade of application. Int J Climatol 33: 1707-1719. http://dx.doi.org/10.1002/joc.3544

Xiong LH, Guo SL (2004) Trend test and change-point detection for the annual discharge series of the Yangtze River at the Yichang hydrological station. Hydrol Sci J 49 (1): 99-112. http://dx.doi.org/10.1623/hysj.49.1.99.53998

Xiong LH, Jiang C, Du T (2014) Statistical attribution analysis of the nonstationarity of the annual runoff series of the Weihe River. Water Sci Technol 70 (5): 939-946. http://dx.doi.org/10.2166/wst.2014.322

Yang T, Li HH, Wang WG, Xu C-Y, Yu ZB (2012) Statistical downscaling of extreme daily precipitation, evaporation, and temperature and construction of future scenarios. Hydrol Process 26: 3510-3523. http://dx.doi.org/10.1002/hyp.8427

Zhang ZX, Chen X, Xu C-Y, Yuan LF, Yong B, Yan SF (2011) Evaluating the non-stationary relationship between precipitation and streamflow in nine major basins of China during the past 50 years. J Hydrol 409(1): 81-93. http://dx.doi.org/10.1016/j.jhydrol.2011.07.041

Zuo DP, Xu ZX, Wu W, Zhao J, Zhao FF (2014) Identification of Streamflow Response to Climate Change and Human Activities in the Wei River Basin, China. Water Resour Manag 28(3): 833-851. http://dx.doi.org/10.1007/s11269-014-0519-0

Table 1 Summary of the distributions used to model the low-flow series in this study

Distribution	Probability density function	Moments	Link functions
Gamma	$f_Z(z \mid \mu,\sigma) = \frac{1}{(\mu\sigma^2)^{1/\sigma^2}} \frac{z^{(1/\sigma^2-1)} e^{-z/(\mu\sigma^2)}}{\Gamma(1/\sigma^2)}$ $z>0, \mu>0, \sigma>0$	$E(Z) = \mu$ $Var(Z) = \mu^2\sigma^2$	$g_1(\mu) = \ln(\mu)$ $g_2(\sigma) = \ln(\sigma)$
Weibull	$f_Z(z \mid \mu,\sigma) = \frac{\sigma z^{\sigma-1}}{\mu^\sigma} \exp\left[-\left(\frac{z}{\mu}\right)^\sigma\right]$ $z>0, \mu>0, \sigma>0$	$E(Z) = \mu\Gamma\left(\frac{1}{\sigma}+1\right)$ $Var(Z) = \mu^2\left\{\Gamma\left(\frac{2}{\sigma}+1\right) - \left[\Gamma\left(\frac{1}{\sigma}+1\right)\right]^2\right\}$	$g_1(\mu) = \ln(\mu)$ $g_2(\sigma) = \ln(\sigma)$
Gumbel	$f_Z(z \mid \mu,\sigma) = \frac{1}{\sigma}\exp\left\{-\left(\frac{z-\mu}{\sigma}\right) - \exp\left[-\frac{(z-\mu)}{\sigma}\right]\right\}$ $-\infty<z<\infty, -\infty<\mu<\infty, \sigma>0$	$E(Z) = \mu+\gamma\sigma \approx \mu+0.57722\sigma$ $Var(Z) = \frac{\pi^2}{6}\sigma^2 \approx 1.64493\sigma^2$	$g_1(\mu) = \mu$ $g_2(\sigma) = \ln(\sigma)$
Logistic	$f_Z(z \mid \mu,\sigma) = \frac{1}{\sigma}\left\{\exp\left[-\left(\frac{z-\mu}{\sigma}\right)\right]\right\}\left\{1+\exp\left[-\left(\frac{z-\mu}{\sigma}\right)\right]\right\}^{-2}$ $-\infty<z<\infty, -\infty<\mu<\infty, \sigma>0$	$E(Z) = \mu$ $Var(Z) = \frac{\pi^2}{3}\sigma^2 \approx 3.28987\sigma^2$	$g_1(\mu) = \mu$ $g_2(\sigma) = \ln(\sigma)$
Lognormal	$f_Z(z \mid \mu,\sigma) = \frac{1}{\sqrt{2\pi}\sigma}\frac{1}{z}\exp\left\{-\frac{\left[\log(z)-\mu\right]^2}{2\sigma^2}\right\}$ $z>0, \mu>0, \sigma>0$	$E(Z) = \omega^{1/2}e^{\mu}$ $Var(Z) = \omega(\omega-1)e^{2\mu}$ $\omega = \exp(\sigma^2)$	$g_1(\mu) = \mu$ $g_2(\sigma) = \ln(\sigma)$

Table 2 Summary of the nonstationary models fitted to the low-flow series of the Wei River using time or meteorological variables as covariates. The critical values of the Filliben correlation coefficient is $F_\alpha = 0.978$ and the KS test is $D_\alpha = 1.36/\sqrt{56} \approx 0.182$, at $\alpha = 0.05$. (a F_r bigger than F_α and a D_{KS} smaller than D_α indicate that the nonstationary model passes the goodness-of-fit test)

Fitted model	**Estimated parameters (standard errors)**	**AIC values**	**Filliben correlation coefficient F_r**	**KS statistic D_{KS}**
Nonstationary Weibull* (EWT interpretation)	$\mu_a = 7.5266(0.1652)$ $\mu_b = -0.0229(0.0066)$ $\sigma_a = 0.7664(0.2600)$ $\sigma_b = -0.0145(0.0082)$	872.4	0.982	0.086
Nonstationary Weibull** (ENE interpretation)	$\mu_a = 14.3504(1.3879)$ $\mu_b = -0.7795(0.1455)$ $\sigma_a = -0.6740(0.2096)$ $\sigma_b = 0.0020(0.0003)$	863.8	0.983	0.074

*Nonstationarities in both the location $\ln(\mu_t) = \mu_a + \mu_b(t+\tau)$ and scale $\ln(\sigma_t) = \sigma_a + \sigma_b(t+\tau)$ parameters with time as covariate. τ is the length of the observed period, in this study $\tau = 56$.

**Nonstationarities in both the location $\ln(\mu_t) = \mu_a + \mu_b T_{ave,t}$ and scale $\ln(\sigma_t) = \sigma_a + \sigma_b Pr_t$ parameters with T_{ave} and Pr as covariates.

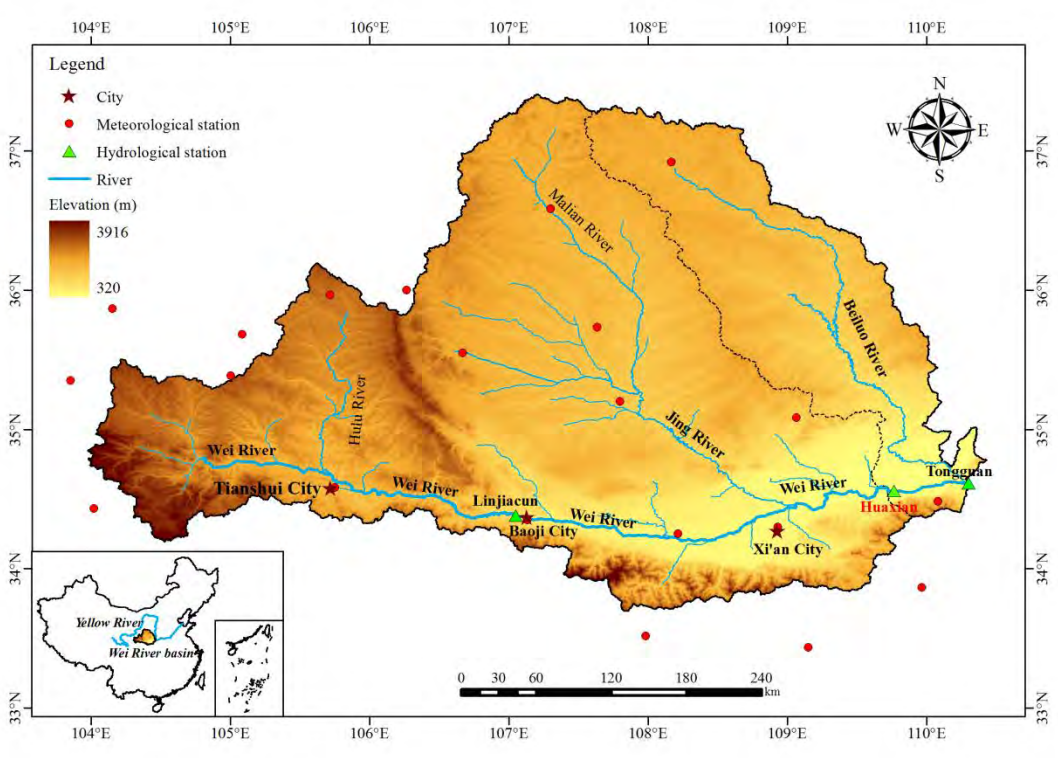

Fig. 1 Location, topography, hydro-meteorological stations and river systems of the Wei River basin

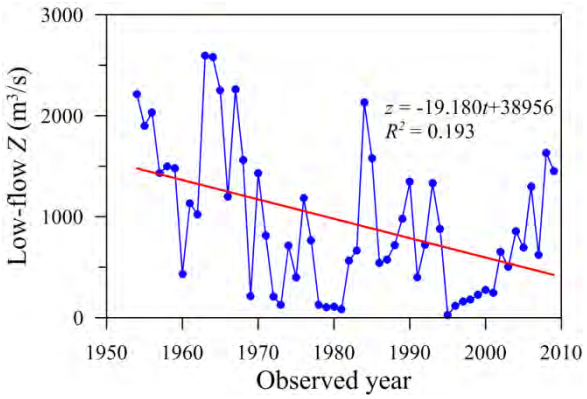

Fig. 2 The observed low-flow series and fitted linear trend for data from Huaxian hydrological station on the Wei River

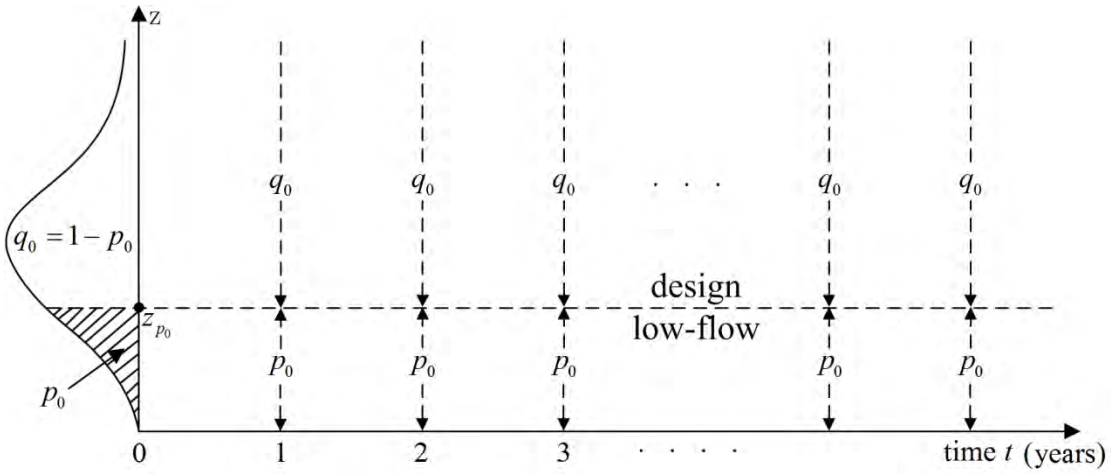

Fig. 3 Schematic depicting the design low-flow quantile z_{p_0} with constant exceedance probability p_0

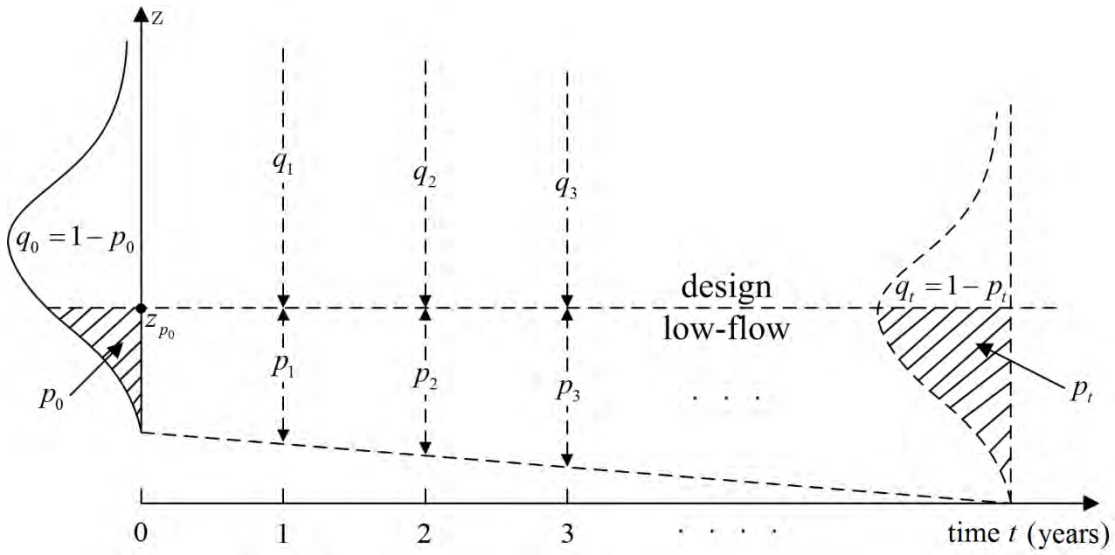

Fig. 4 Schematic depicting the design low-flow quantile z_{p_0} with time-varying exceedance probabilities $p_t, t = 1, 2, ..., \infty$

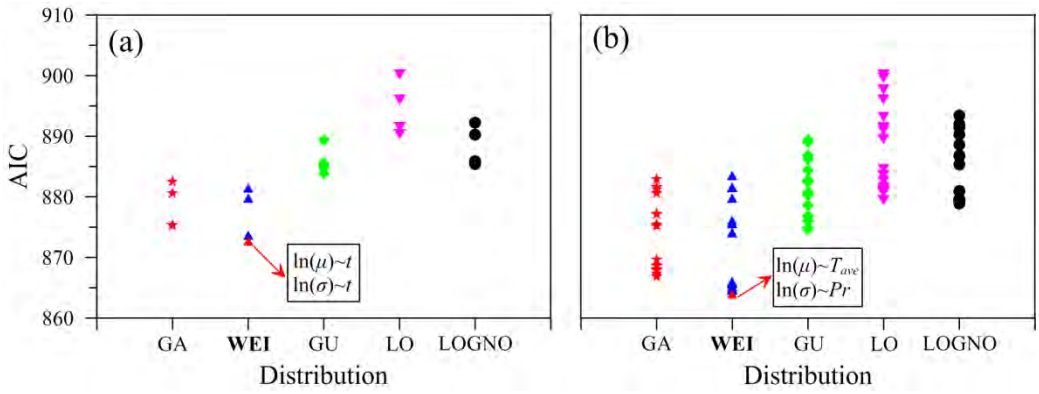

Fig. 5 Summary of different distributions with different nonstationary models fitted to the observed low-flow series. Location μ and scale σ parameters modeled as functions of (a) time, and (b) meteorological variables T_{ave} and Pr. The expressions in the black box is the optimal nonstationary model for respective case of covariate analysis

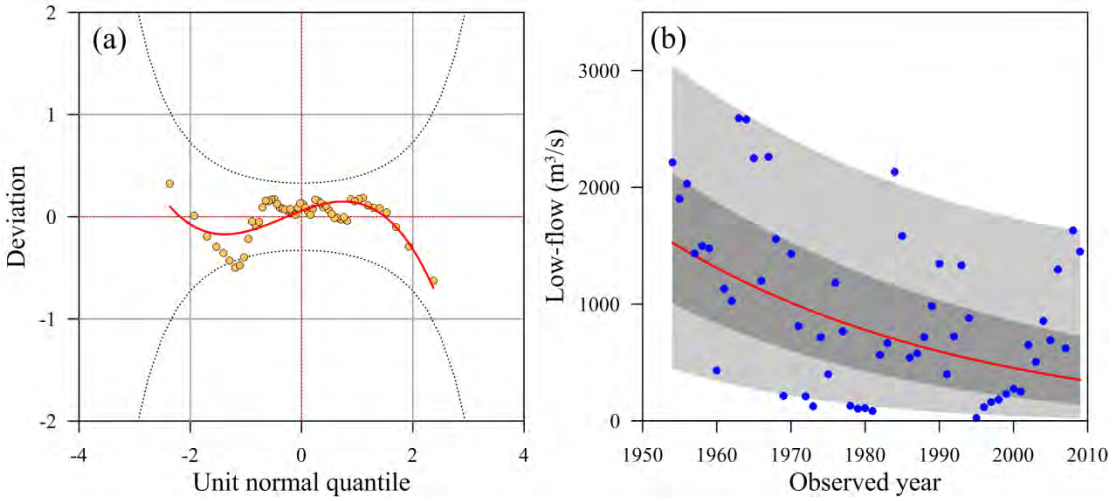

Fig. 6 Diagnostic plots for assessing the performance of the optimal nonstationary model using time as covariate: (a) Worm plot (for a good fit, the data points should be aligned preferably along the red solid line but within the 95% confidence intervals indicated by the two grey dashed lines); (b) Centile curves plot (the blue points are the observed low-flow series, the red line is the 50% centile curve, the dark grey region is the area between the 25% and 75% centile curves and the light grey region is the area between the 5% and 95% centile curves)

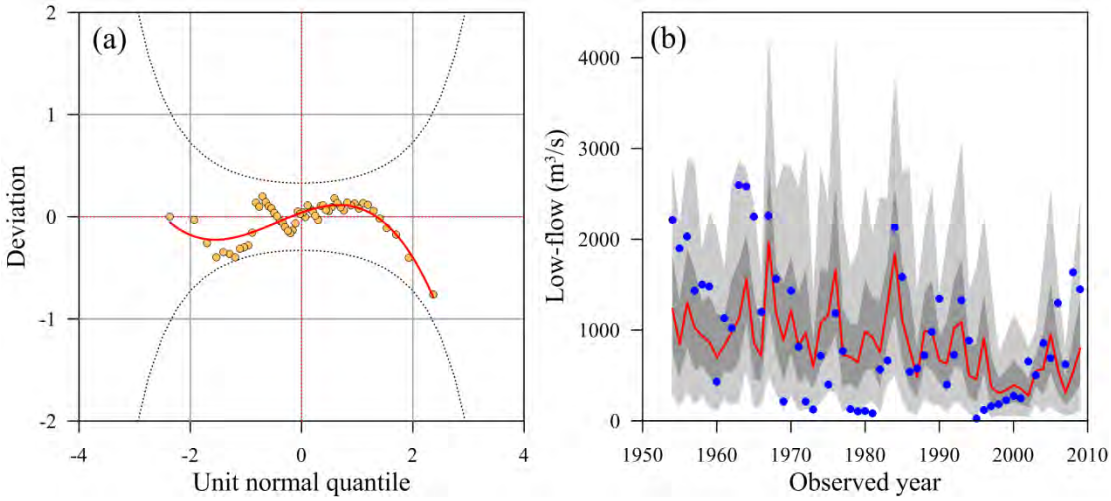

Fig. 7 Diagnostic plots for assessing the performance of the optimal nonstationary model using meteorological variables T_{ave} and Pr as covariates: (a) Worm plot (for a good fit, the data points should be aligned preferably along the red solid line but within the 95% confidence intervals indicated by the two grey dashed lines); (b) Centile curves plot (the blue points are the observed low-flow series, the red line is the 50% centile curve, the dark grey region is the area between the 25% and 75% centile curves and the light grey region is the area between the 5% and 95% centile curves)

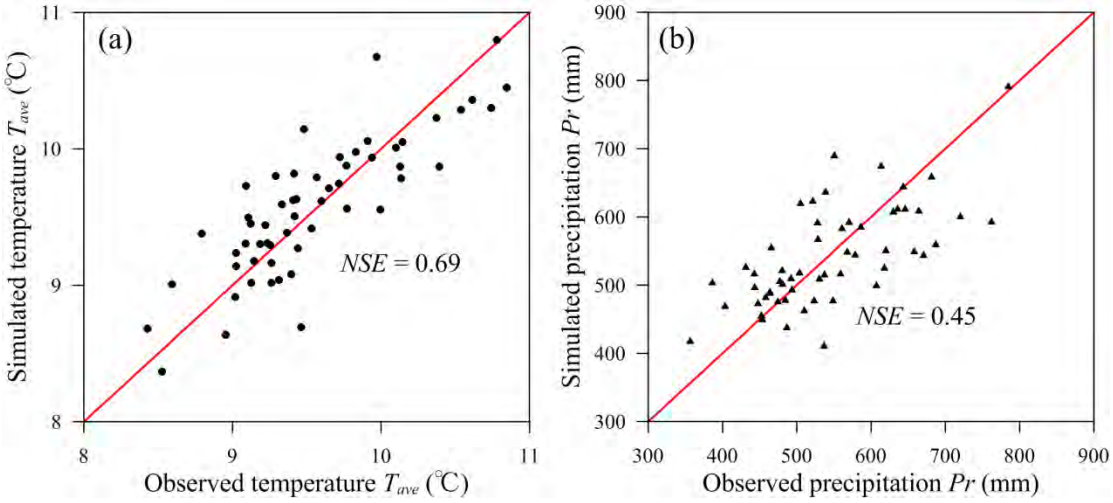

Fig. 8 Comparisons between simulated and observed meteorological variables for the observed period 1954-2009: (a) Annual average temperature T_{ave} (℃); (b) Annual total precipitation Pr (mm). Both variables were simulated by the weather generator in the SDSM driven by the NCEP reanalysis predictors

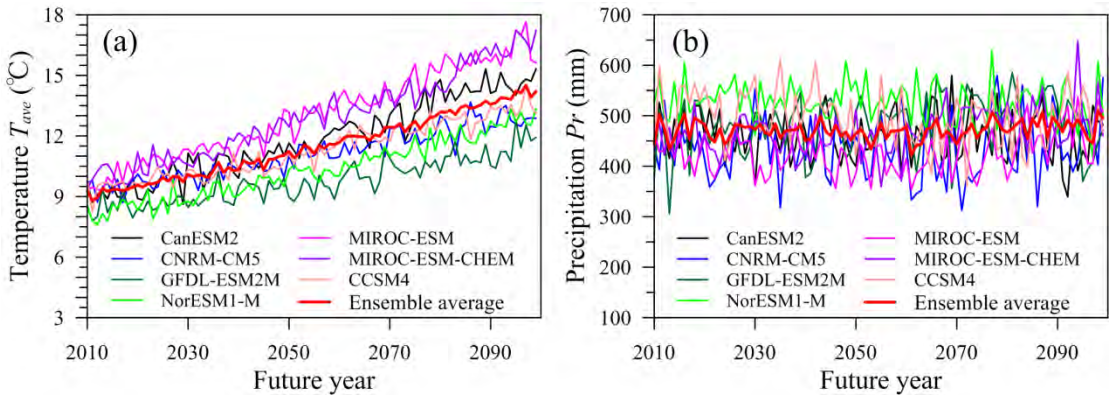

Fig. 9 Projected meteorological variables from different GCM models for the future period 2010-2099. The Ensemble average is the arithmetic average value of all the individual GCM models: (a) Annual average temperature T_{ave} (℃); (b) Annual total precipitation Pr (mm)

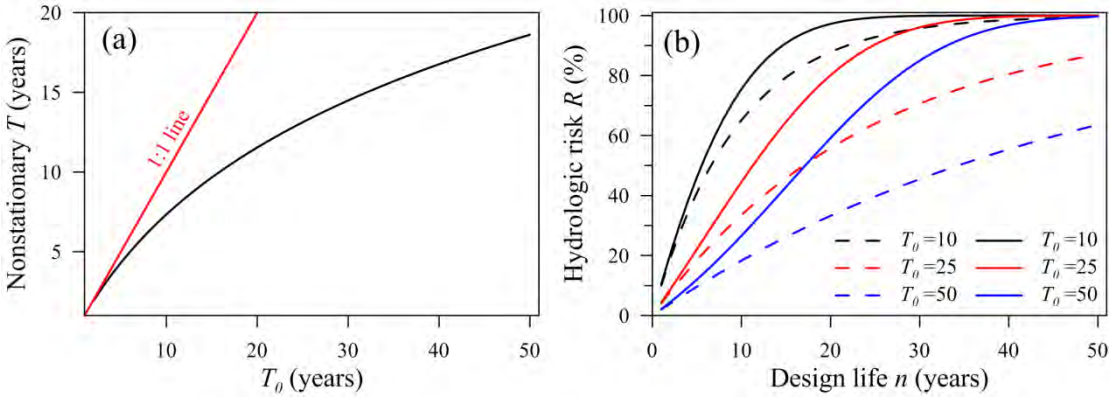

Fig. 10 Nonstationary return period T and hydrological risk R of the Wei River design low-flow quantile z_{P_0} (corresponding to the initial return period T_0) under the EWT interpretation: (a) Relation of the nonstationary return period T and the initial return period T_0; (b) Nonstationary hydrological risk R as a function of design life n for z_{P_0} with different initial return periods T_0 (the dashed lines are the risk under stationary conditions and the solid lines are the risk under nonstationary conditions)

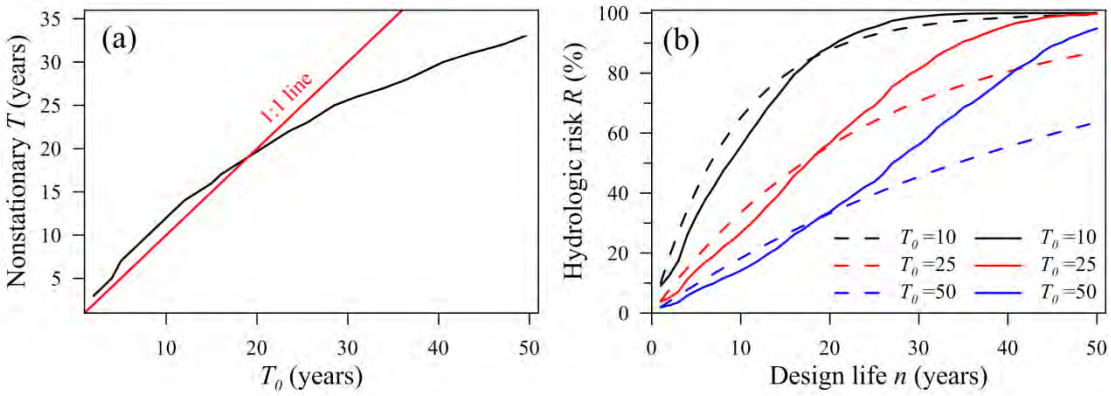

Fig. 11 Nonstationary return period T and hydrological risk R of the Wei River design low-flow quantile z_{P_0} (corresponding to the initial return period T_0) under the ENE interpretation: (a) Relation of the nonstationary return period T and the initial return period T_0; (b) Nonstationary hydrological risk R as a function of design life n for z_{P_0} with different initial return periods T_0 (the dashed lines are the risk under stationary conditions and the solid lines are the risk under nonstationary conditions). Because of the inverse solving of Eq. 10 and use of meteorological covariates, the nonstationary T and R are not as smooth as the EWT case

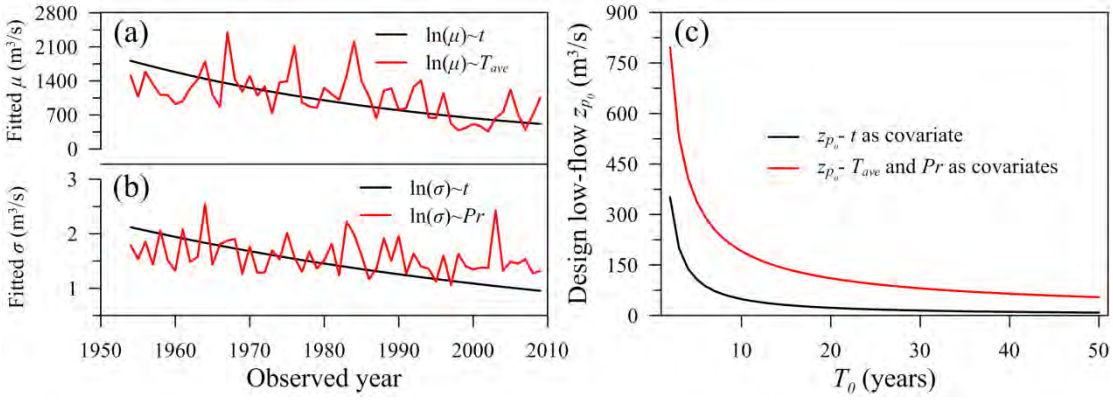

Fig. 12 Results of the fitted statistical parameters μ, σ and design low-flow quantile z_{P_0} by two nonstationary models with different covariates, one is the optimal nonstationary model using time as covariate (black lines), and the other is the optimal nonstationary model using T_{ave} and Pr as covariates (red lines). Fitted (a) location μ and (b) scale σ parameters of the low-flow distribution for the observed period; (c) Design low-flow quantile z_{P_0} for the initial year $t = 0$ corresponding to different initial return periods $T_0 = 2, 3, ..., 50$